Binary and ternary NiTi-based shape memory films deposited by simultaneous sputter deposition from elemental targets

S. Sanjabi[a)]
Department of Materials Science & Metallurgy, Device Materials Group, Cambridge University, Pembroke Street, Cambridge CB2 3QZ, United Kingdom and Department of Materials Science and Engineering, Sharif University of Technology, P.O. Box 11365-9466,Tehran, Iran

Y. Z. Cao
Shanghai Institute of Ceramics, Chinese Academy of Sciences,1295 Dingxi Road, Shanghai 200050, China

S. K. Sadrnezhaad
Department of Materials Science and Engineering, Sharif University of Technology P.O. Box 11365-9466, Tehran, Iran

Z. H. Barber
Department of Materials Science & Metallurgy, Device Materials Group, Cambridge University, Pembroke Street, Cambridge CB2 3QZ, United Kingdom

(Received 22 March 2005; accepted 5 July 2005)

The most challenging requirement for depositing NiTi-based shape memory thin films is the control of film composition because a small deviation can strongly shift the transformation temperatures. This article presents a technique to control film composition via adjustment of the power supplied to the targets during simultaneous sputter deposition from separate Ni, Ti, and X (e.g., Hf) targets. After optimization of sputter parameters such as working gas pressure, target-substrate distance, and target power ratio, binary $Ni_{100-x}Ti_x$ thin films were fabricated and characterized by energy dispersive x-ray spectroscopy in a scanning electron microscope (to measure the film composition and uniformity), *in situ* x-ray diffraction (to identify the phase structures), and differential scanning calorimetry (to indicate the transformation and crystallization temperatures). To explore the possibility of depositing ternary shape memory NiTi-based thin films with a high temperature transformation $>100\,^{\circ}C$, a Hf target was added to the NiTi deposition system. Annealing was carried out in a high vacuum furnace slightly above the films' crystallization temperatures (500 and 550 °C for NiTi and NiTiHf films, respectively). Differential scanning calorimetry (DSC) results of free-standing films illustrated the dependence of transformation temperatures on film composition: Ap and Mp (referring to the austenitic and martensitic peaks in the DSC curve) were above room temperature in near equiatomic NiTi and Ti-rich films, but below it in Ni-rich films. In NiTiHf films, the transformation temperatures were a function of Hf content, reaching as high as 414 °C (Ap) at a Hf content of 24.4 at. %. Atomic force microscopy revealed nanostructure surface morphology of both NiTi and NiTiHf films. Detailed characterization showed that the film properties were comparable with those of NiTi and NiTiHf bulk alloys. © *2005 American Vacuum Society.* [DOI: 10.1116/1.2011404]

I. INTRODUCTION

The basic phenomenon of the shape memory effect is the martensitic phase transition between relatively high-temperature, high symmetry austenite phase and low-temperature, low symmetry martensite, such that the deformed alloy can revert back to its original shape when heated above its transition temperature.[1] This unique property and additional excellent superelasticity and biocompatibility have led to considerable interest in NiTi-based shape memory alloys for functional applications at low (e.g., NiTi $<100\,^{\circ}C$) and high (e.g., NiTiHf $>100\,^{\circ}C$) temperature.[2,3] Growth of shape memory alloys (SMAs) in thin film form improves high response actuation during thermal cycling and opens applications in microelectromechanical systems (MEMS) and Bio-MEMS.[4,5]

Fabrication of SMA thin films is commonly performed by rf or dc magnetron sputtering.[6] However, deposition of useful shape memory material is often problematic due to different sputtering yields of depositing elements which cause compositional deviation between alloy target and deposited film (NiTi-based alloys are very sensitive to composition variation and 1 at. % deviation near the equiatomic composition can shift the transformation by around 100 °C).[7] For example, sputtering of NiTi thin films from an equiatomic NiTi alloy target invariably leads to Ni-rich films (films may be Ti poor with respect to the target by around 2–4 at. %) because the sputtering yield for Ni is higher than that for

a)Author to whom correspondence should be addressed; present address: Dept. of Materials Science and Engineering, Sharif University of Technology, P. O. Box: 11365-9466, Tehran-Iran; electronic mail: sanjabi@mehr.sharif.edu

Ti.[8,9] This problem is exacerbated in ternary alloy films deposited from an alloy target: Johnson *et al.*[10] deposited NiTiHf films from an alloy target, and these showed no transformation behavior above room temperature after annealing, probably due to an excess of nickel. The simplest and most common solution to this composition problem is to place small pieces of pure Ti (or the third component, *X*, e.g., Hf) onto the wear track of the binary or ternary NiTi (*X*) target to compensate for the increased Ni sputtered flux.[6,10] Alternatively this can be achieved by cosputtering of the alloy target with the required element as an additional target,[4,11] using a manufactured alloy target enriched in the deficient component(s),[12] or varying the working gas pressure in the chamber.[13] However, target modification generally requires a trial and error approach to produce the correct film composition: the composition adjustment using Ti or Hf plates requires control of numerous parameters such as number, geometry, size and position, and any subsequent change of the deposition parameters will require readjustment. It is also difficult to adjust the composition by varying Ar gas pressure because at high pressures films become brittle, with poor structure.[14] Manufacture of the required alloy targets by investment casting or powder metallurgy requires careful control of impurities such as oxygen, or prealloyed powder impurities.[15] Manufacturing a sputtering target from the as-cast (e.g., NiTiHf) alloy may also be difficult because the alloys are brittle (e.g., for high Hf content).[16]

We have used a method to fabricate binary $Ni_{100-x}Ti_x$ and ternary $Ni_{50}Ti_{50-x}Hf_x$ films by simultaneous deposition from separate pure Ni, Ti, and Hf targets, controlling the film composition by adjusting the ratio of powers supplied to each target. This technique is cost effective (fabrication from pure elements), can easily be optimized under varying sputtering parameters, and can be developed to deposit other ternary shape memory thin films. Results show that the film quality is comparable with bulk material.

II. FABRICATION PROCEDURE

NiTi films were deposited by ultrahigh vacuum dc magnetron sputtering onto unheated Si (100) substrates of dimension 10 mm × 5 mm. The deposition system allowed three magnetrons (target size: 35 mm × 55 mm), plus associated heater leads, instrumentation feedthroughs, viewing port, and rotary shaft to be placed on one standard 200 mm o.d. flange, inserted into a 150 mm i.d. nitrogen-cooled can.[17] Configuration of the targets used in this study is shown schematically in Fig. 1, with three targets (Ni, Ti, and Hf with a purity of 99.9%) and a substrate support which was rotated in the horizontal plane during film deposition in order to achieve a uniform film composition. The power to each target was controlled precisely by computer. A base vacuum of $<10^{-6}$ Pa was achieved after overnight bakeout and subsequent liquid nitrogen cooling of the chamber walls prior to deposition. A constant flow of Ar (99.999%) was controlled with a leak valve during film deposition, and various sputtering gas pressures (~0.6–1.2 Pa) were set by throttling the gate valve.

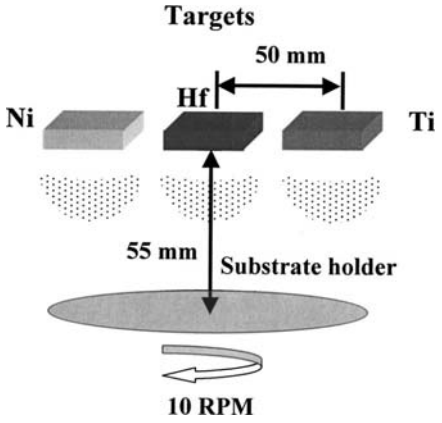

FIG. 1. Schematic sputtering configuration.

Without substrate rotation, and at a target-substrate distance of 55 mm, a composition variation around 0.5 at. % per mm was produced across a single substrate (this variation was inversely proportional to the target-substrate distance). With rotation of the substrate support at 10 rpm a uniformity around 0.01 at. % per mm was obtained.[18]

A range of Ar sputtering gas pressures between 0.6 and 1.2 Pa was used to explore the effect of working gas pressure on the film microstructure and shape memory properties. Following deposition at high Ar gas pressure, the as-deposited films were brittle and easily fractured.

Figure 2 shows the film composition as a function of applied power to each target in binary and ternary systems. The composition of as-deposited films was determined by electron dispersive x-ray spectroscopy using a JEOL JSM-5800LV operating at 15 keV. In the binary NiTi system, Fig. 2(a), the applied power to the Ni target was kept at 27 W and, by changing the Ti power from 95 to 85 W, film compositions varying from Ti-rich, to near equiatomic and Ni-rich were achieved. Figures 2(b) and 2(c) show the results of adding Hf to the optimized near-equiatomic NiTi films. By increasing Hf power and decreasing Ti, the Ti content of the film was replaced by Hf. These results were obtained at a constant target-substrate distance of 55 mm and a working gas pressure of 0.6 Pa.

The thickness of the films was measured by surface profilometry (Talysurf 6, Taylor-Hobson) using the step height on a masked silicon substrate: the thickness of the films was around 2 μm, the deposition rate was calculated to be ~1 μm/h. As-deposited films were subsequently annealed in a vacuum furnace (base pressure $<10^{-5}$ Pa with heating and cooling rates of approximately 50 °C/min. A Siemens D500 x-ray diffractometer (XRD) with Cu Kα(λ = 1.54056 Å)) x-ray source, equipped with temperature control was used to identify the film structure as a function of temperature. Differential scanning calorimetry (DSC) (Q1000, TA instrument, with the minimum required mass =0.5 mg) was used to indicate the crystallization temperature and transformations at heating and cooling rates of 10 °C/min. The surface morphology of the films was deter-

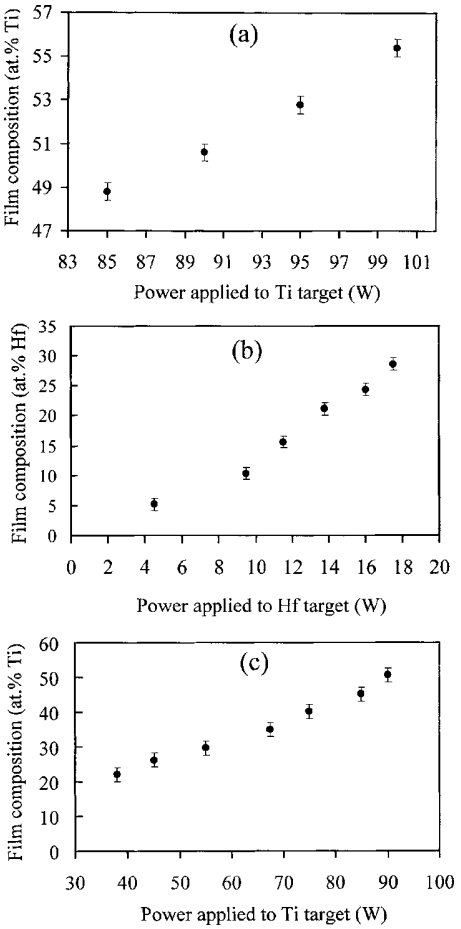

FIG. 2. Film composition as a function of applied power to the targets (the power of Ni was kept at 27 W): (a) for $Ni_{100-x}Ti_x$ films; (b) and (c) for $Ni_{50}Ti_{50-x}Hf_x$ films.

mined by atomic force microscopy (AFM) (Digital Instruments Nanoscope III) under contact mode at room temperature.

III. RESULTS AND DISCUSSION

The as-deposited films exhibited no crystalline XRD peaks, suggesting an amorphous structure. A broad peak around $2\theta=42°$ and 40 ° was observed for NiTi and NiTiHf films, respectively, indicating that the structure is expanded by introducing Hf into the NiTi binary system.

To find an appropriate annealing temperature for crystallization of the as-deposited films, a DSC measurement was made after peeling the films from their Si substrates. Figure 3 shows the crystallization temperature: for an equiatomic NiTi film this was around 472 °C and for $Ni_{49.5}Ti_{34.9}Hf_{15.6}$ it was 502 °C. The crystallization temperature of NiTiHf was dependent upon the Hf content, increasing to 519 °C with increasing atomic percent of Hf (to 28.7 at. %). More details are given in Ref. 19.

Based on these DSC results, the as-deposited films were annealed in a high vacuum furnace at 500 °C for NiTi films and 550 °C for NiTiHf for 1 h. Figures 4(a) and 4(b) show

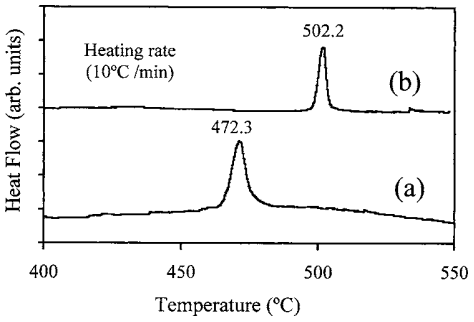

FIG. 3. Crystallization temperature evaluation of: (a) near-equiatomic $Ni_{49.4}Ti_{50.6}$ and (b) $Ni_{49.5}Ti_{34.9}Hf_{15.6}$ films.

the room temperature XRD patterns of annealed NiTi and NiTiHf films, respectively. The peak positions show that at room temperature the phase structure of both NiTi and $Ni_{49.5}Ti_{34.9}Hf_{15.6}$ annealed films corresponds to monoclinic martensitic structure (by comparison with monoclinic structure of NiTi from XRD source data file No. 35-1281). The peak positions and intensity of the NiTiHf film are slightly different from those of the NiTi film. The lattice parameters a,b,c, and the monoclinic angle β were calculated for NiTi as 2.89, 4.11, 4.62 Å, and 97.07° respectively, while those for NiTiHf with 15.6 at. % Hf were 3.01, 4.07, 4.79 Å, and 101.86°, similar to the reported data for (15 at. %) NiTiHf bulk alloy.[20] These results indicate that the Hf addition causes an increase of a,c, and β, and a decrease of b.

Figures 4(c) and 4(d) show XRD spectra of a NiTi film at 100 °C and NiTiHf at 200 °C, respectively, indicating the presence of a parent austenite phase at higher temperatures. During heating, the room temperature monoclinic martensitic structure transforms to the cubic austenitic phase in both films. The austenitic peaks of these films are not in the same position, indicating that Hf additions lead to an expanded austenitic lattice (a=3.01 Å for NiTi and 3.08 Å for 15.6 at. % Hf).

Figures 5(a) and 5(b) show the DSC plots of NiTi and NiTiHf films, respectively, revealing the phase transformation behavior associated with the shape memory effect. Both the heating and cooling curves demonstrate a single endotherm and double exotherm, indicating the presence of *R*

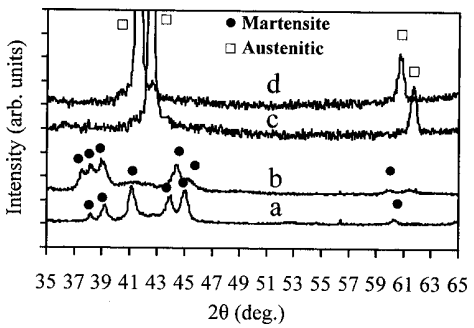

FIG. 4. XRD trace of crystallized films: (a) $Ni_{49.4}Ti_{50.6}$ at room temperature (RT), (b) $Ni_{49.5}Ti_{34.9}Hf_{15.6}$ at RT, (c) $Ni_{49.4}Ti_{50.6}$ at 100 °C, and (d) $Ni_{49.5}Ti_{34.9}Hf_{15.6}$ at 200 °C.

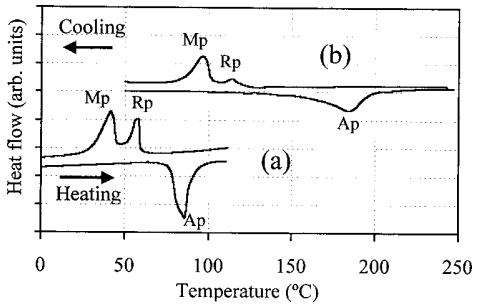

FIG. 5. DSC plots of: (a) near-equiatomic $Ni_{49.4}Ti_{50.6}$ film and (b) $Ni_{49.5}Ti_{34.9}Hf_{15.6}$.

phase during phase transformation in both films. In the NiTi film, during heating, the downward endothermic peak (Ap) corresponds to the transformation to the austenitic phase, for which the transformation starts from 71 °C and finishes at 86 °C. During cooling two upward exothermic peaks (Rp and Mp) correspond to transformation from austenitic to the intermediate rhombohedral *R*, phase structure[1] followed by martensitic structure at room temperature. In NiTiHf the transformation steps are similar, but occur at higher temperature and over a wider temperature range, confirming a wider hysteresis loop for NiTiHf alloys. The occurrence of the austenitic transformation (Ap) above 150 °C illustrates the transformation temperature increase with increasing Hf content.

Figure 6 shows the phase transformation temperatures (for Ap and Mp) as a function of composition for both binary NiTi and ternary NiTiHf thin films. In Fig. 6(a) the transformation temperatures are seen to be very sensitive to Ti content: deviation of around 1 at. % from near equiatomic composition causes the transformations to take place below room temperature [e.g., a Ti content of 48.8 at. % had a martensitic transformation (Mp) around −50 °C]. Similar results have been reported elsewhere for NiTi bulk material.[7] As can be seen from Fig. 6(b), by adding Hf the transformation temperatures are at first decreased (below 5 at. % Hf), but for higher Hf additions, the transformation temperatures are increased considerably. An austenitic transformation temperature (Ap) around 414 °C is achieved by replacing Ti in NiTiHf with Hf content about 24.4 at. %. For NiTiHf alloy, it has been reported elsewhere that the transformation temperatures increase with increase in the Hf content and that the highest phase transformation temperature (above 500 °C) is reached with a Hf content of around 30 at. %.[21,22]

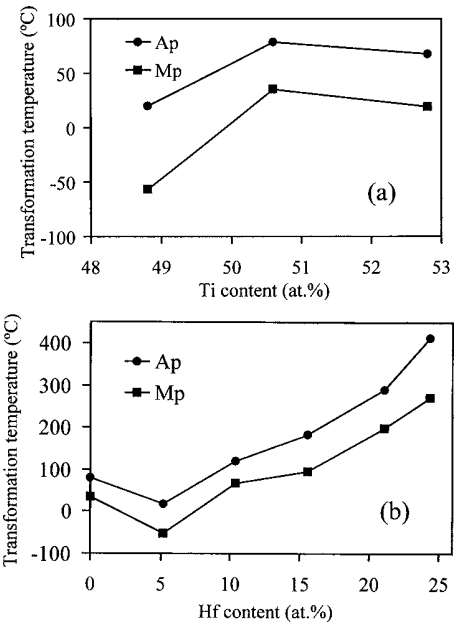

FIG. 6. Transformation temperature as a function of composition: (a) $Ni_{100-x}Ti_x$ binary and (b) $Ni_{50}Ti_{50-x}Hf_x$ (Mp and Ap refer to exothermic and endothermic peaks in the DSC graph).

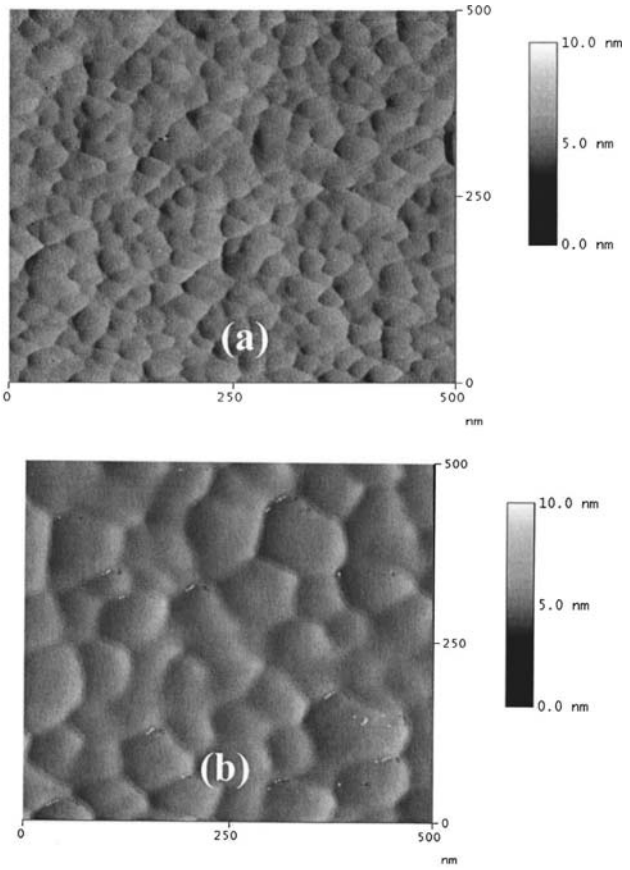

FIG. 7. AFM surface images of: (a) near-equiatomic $Ni_{49.4}Ti_{50.6}$ and (b) $Ni_{49.5}Ti_{34.9}Hf_{15.6}$.

Figure 7 shows the AFM micrographs of both NiTi and NiTiHf film surface morphology. As can be seen in this figure, the surface feature size of the NiTi film is <100 nm while that of the NiTiHf is ~ 100 nm. This difference in surface morphology may reflect the different annealing temperatures (higher in the case of the NiTiHf). The crystalline domain size for the films was also estimated to be <100 nm from the width of the austenitic XRD peaks at high temperatures, assuming that they are free from nonuniform strains, using the Scherrer formula.[23] Recent studies have shown that fine grain structures in thin films may lead to significantly

different transformation temperature from those of corresponding bulk coarse-grained samples due to suppressed martensitic transformation in fine crystalline grains.[24,25] However, our results show that the shape memory effect can be achieved in both binary NiTi and ternary NiTiHf thin films with grain sizes of ~100 nm.

IV. CONCLUSION

A technique was explored to deposit binary and ternary NiTi-based shape memory thin films using simultaneous sputter deposition from separate elemental targets. Characterization of films of varying composition was carried out using XRD and DSC. Transformation temperatures were shown to be a function of film composition: in NiTi films the transformation temperature was sensitive to composition around the equiatomic Ni/Ti ratio, and Hf additions led to austenitic transformation temperatures (Ap) up to 414 °C at 24.4 at. % Hf. The advantages of this method are the ability to control the film composition precisely with any chosen sputtering parameters, and the lack of a requirement to fabricate binary, or ternary, alloy targets.

ACKNOWLEDGMENT

The authors would like to thank Dr. Nadia Stelmashenko for her help with AFM.

[1]K. Otsuka and X. Ren, Prog. Mater. Sci. **50**, 511 (2005).
[2]Y. Fu, H. Du, W. Huang, S. Zhang, and M. Hu, Sens. Actuators, A **112**, 395 (2004).
[3]D. S. Grummon, JOM **55**, 24 (2003).
[4]C. L. Shih, B. K. Lai, H. Kahn, S. M. Philips, and A. H. Heuer, J. MEMS **10**, 69 (2001).
[5]J. J. Gill, D. T. Chang, L. A. Momoda, and G. P. Carman, Sens. Actuators, A **93**, 148 (2001).
[6]S. Miyazaki and A. Ishida, Mater. Sci. Eng., A **273–275**, 106 (1999).
[7]K. N. Melton, *Engineering Aspects of Shape Memory Alloys* (Butterworth-Heinemann, London, 1990), p. 23.
[8]D. S. Grummon, L. Hou, Z. Zhao, and T. J. Pence, J. Phys. IV **5**, 665 (1995).
[9]V. Martynov, A. D. Johnson, and V. Gupta, J. Phys. IV **112**, 845 (2003).
[10]A. D. Johnson, V. V. Martynov, and R. S. Minners, J. Phys. IV **5**, 783 (1995).
[11]H. Du and Y. Fu, Surf. Coat. Technol. **176**, 182 (2004).
[12]E. Quandt, C. Halene, H. Holleck, K. Feit, M. Kohl, P. Schlomacher, and A. Skokan, Sens. Actuators, A **53**, 434 (1996).
[13]A. Ohta, S. Bhansali, I. Kishimoto, and A. Umeda, Sens. Actuators, A **86**, 165 (2000).
[14]A. Ishida, A. Takei, and S. Miyazaki, Thin Solid Films **228**, 210 (1993).
[15]H. Rumpf, B. Winzek, C. Zamponi, W. Siegert, K. Neuking, and E. Quandt, Mater. Sci. Eng., A **378**, 249 (2004).
[16]S. Besseghini, E. Villa, and A. Tuissi, Mater. Sci. Eng., A **273–275**, 390 (1999).
[17]R. E. Somekh and Z. H. Barber, J. Phys. E **21**, 1029 (1988).
[18]S. Sanjabi, S. K. Sadrnezhaad, K. A. Yates, and Z. H. Barber (unpublished).
[19]S. Sanjabi, Y. Z. Cao, and Z. H. Barber, Sens. Actuators, A **121**, 543 (2005).
[20]P. L. Potapov, A. V. Shelyakov, A. A. Gulyaev, E. L. Svistunova, N. M. Matveeva, and D. Hodgson, Mater. Lett. **32**, 247 (1997).
[21]D. R. Angst, P. E. Thoma, and M. Y. Kao, J. Phys. IV **5**, 747 (1995).
[22]D. N. AbuJudom, P. E. Thoma, M. Y. Kao, and D. R. Angst, U.S. Patent No. 5,114,504 (1992).
[23]B. D. Cullity and S. R. Stock, *Elements of X-ray Diffraction*, 3rd ed. (Prentice–Hall, Upper Saddle River, N.J., 2001), p.167.
[24]H. D. Gu, K. M. Leung, and C. Y. Chung, J. Vac. Sci. Technol. A **16**, 3420 (1998).
[25]E. Cesari, P. Ochin, R. Portier, V. Kolomytsev, Y. Koval, A. Pasko, and V. Soolshenko, Mater. Sci. Eng., A **273–275**, 738 (1999).